Performance of Machine Learning Aided Fluid Antenna System with Improved Spatial Correlation Model

Zhi Chai[1], Kai-Kit Wong[1], Kin-Fai Tong[1], Yu Chen[2], and Yangyang Zhang[3]
[1]Department of Electronic and Electrical Engineering, University College London, London, United Kingdom
[2]School of Information and Communication Engineering, Beijing University of Posts and Telecommunications, Beijing, China
[3]Kuang-Chi Science Limited, Hong Kong SAR, China

***Abstract*—Fluid antenna has emerged as a new antenna technology that enables software-controllable position reconfigurability for great diversity and multiplexing benefits. The performance of fluid antenna systems has recently been studied for single and multiuser environments adopting a generalized spatial correlation model that accounts for the channel correlation between the ports of the fluid antenna. The recent work [1] further devised machine learning algorithms to select the best port of fluid antenna in a more practical setting in which only a small number of ports is observable in the selection process, and found that extraordinary outage probability performance can be obtained. However, there is a concern of how the spatial correlation parameters are set to reflect the actual correlation structure for accurately evaluating the system performance. In this paper, the method in [2] is used to set the correlation parameter so that the model can accurately characterize the correlation amongst the ports of a fluid antenna in a given space. This paper revisits the port selection problem for single-user fluid antenna system where learning-based algorithms are employed to select the best port when only a small subset of the channel ports are known. The new results demonstrate that the impact of spatial correlation on the performance becomes more pronounced but the machine learning aided fluid antenna system is still able to match the performance of maximum ratio combining (MRC) system with many uncorrelated antennas.**

***Index Terms*—Fluid antenna, Machine learning, Port selection, Selection combining, Spatial correlation, Outage probability.**

I. Introduction

WIRELESS communications has continued to advance at a rapid rate and 5G (the fifth generation) is the latest edition to impact on how we live and work, and to create new opportunities for people, businesses and society. Regardless of how mobile communications technologies have evolved, it has always been to enhance reliability and the network capacity. The former concerns the receiver's ability to decode fast data in the presence of noise and fading whereas the latter demands the network to accommodate as many users as possible on the same radio channel. Numerous diversity techniques have been developed in recent years to achieve these goals.

Space diversity, which takes advantage of the independency of the channels at distributed antennas, is particularly effective for slow fading channels in which channel coding relying on time diversity fails to work. Switching combining (SC) and maximum ratio combining (MRC) are two of the most popular diversity schemes that have demonstrated promising reception performance when multiple antennas can be used. Evidently, multiple antenna technologies have now become dominated by multiple-input multiple-output (MIMO) systems.

In 5G, the number of antennas at a base station (BS) has been increased to 64 antennas to realize the massive version of MIMO but the same increase in the number of antennas at a mobile device, or user equipment (UE), is not seen. This is hardly surprising because the space in a UE is limited. While there is a tendency to move up the frequency bands for more bandwidth and smaller sized antennas, it helps little in fitting many antennas at the UE since the rule of thumb is to require the antenna spacing to be at least 0.5λ with λ the wavelength of communication. This rule comes about to ensure sufficient channel diversity and avoid any issue due to mutual coupling.

To overcome the 'half-λ' limitation, one emerging technology of great interest is *fluid antenna* [3], [4]. Fluid antenna represents any radiating structure based on software-controllable fluidic, conductive or dielectric element that can change their shape, size and position to reconfigure the polarization, operating frequency, radiation pattern, and other characteristics for radio communications. It also include designs which involve no fluidic materials (e.g., switchable pixels instead) if they can emulate the agility. The term 'fluid antenna' first appeared in [5] where water and chemicals were investigated as potential materials for an antenna using both computer simulations and experiments. Nonetheless, using liquid structures to design an antenna can be traced back to as early as 2004 when mercury was adopted [6]. In 2016, Mitsubishi Electric made headlines for the world's first seawater antenna that shoots a column of seawater to create a plume as an antenna achieving a radiation efficiency of 70% [7]. Such high-profile success provides a strong endorsement for fluid-like antenna from the industry.

Another famous example worth mentioning is the advanced saltwater-based antenna system developed by a research group from Nanjing University of Aeronautics and Astronautics in China that illustrated 360-degree beam-steering for frequencies between 334 to 488MHz [8], [9]. Many reconfigurable fluid antennas have at the same time been developed in recent years

This work is supported in part by the Engineering and Physical Sciences Research Council (EPSRC) under grant EP/T015985/1.

[10]–[15]. On the other hand, reconfigurable pixels using RF MEMS switches have also emerged that could enable delay-free reconfigurability of fluid antenna [16]–[20]. An up-to-date review on liquid-based antennas can be found in [21].

Following the advances in fluid antenna technologies, Wong *et al.* conducted several performance analysis for single [22], [23] and multiuser communication systems [24], [25] employing fluid antennas. In particular, the studies hypothesized the scenarios in which a UE (or all the UEs in the multiuser case) is equipped with a single RF-chain fluid antenna which has the ability to switch its position (referred to as 'port') instantly for maximizing the received signal-to-noise ratio (SNR) or the signal-to-interference ratio (SIR) for multiple access. Results in [22]–[25] indicated that extraordinary diversity and multiplexing gains can be obtained if the number of ports, N, is large. Such impressive performance is supported by the recent surface-wave based fluid antenna design which makes possible a very high-resolution fluid antenna in practice [26].

While the work in [26] suggests that a large-N fluid antenna may be practically feasible, the practicality of fluid antenna is also subjected to whether it is possible to estimate that large number of channel envelopes for port selection. This problem was addressed in [1] by considering the setting where only a small subset of the ports are observed before port selection. It is worth pointing out that the port selection problem differs from the traditional SC problem in that it involves a very large number of ports for selection based on limited observations, and strong channel correlation due to high density of the ports. A combination of machine learning methods including Smart, 'Predict and Optimize' (SPO) [27] was proposed. The results in [1] illustrated that the machine learning aided fluid antenna system can match or even outperform multi-antenna SC and MRC systems with many uncorrelated antennas.

Recently in [2], nevertheless, it was reported that the way the spatial correlation among the ports was modelled in [1], [22]–[24] might underestimate the impact of the size of fluid antenna and could overestimate the achievable performance when the size is small. Though the promising performance of fluid antenna systems was then confirmed using an improved spatial correlation model in [2], whether the machine learning assisted fluid antenna system would perform well, remains a mystery. This prompts us to assess the machine learning based algorithms in [1] using the spatial correlation model in [2]. As a summary of the results, we will show that SPO remains the best approach for port selection. In addition, the performance of a $\frac{\lambda}{2}$-sized fluid antenna does show an obvious degradation although it can still exceed the performance of 3-antenna MRC and 6-antenna SC systems. By contrast, for 2λ and 5λ sized fluid antennas, they seem to have no performance drop.

II. Fluid Antenna System

A. System Model

In this paper, as in [1], we consider a single-user point-to-point system where the transmitter uses a standard antenna to transmit information to a UE equipped with a fluid antenna of size $W\lambda$ where W is the normalized antenna size. The fluid antenna has N ports, spreading evenly over its size, and is assumed to switch to the best port instantly for communications. For flat fading channels, the received signal at the k-th port (with time index omitted) is given by

$$z_k = g_k s + \eta_k, \tag{1}$$

where g_k represents the complex channel at the k-th port, η_k is the zero-mean complex Gaussian noise at the k-th port with variance of σ_η^2, and s denotes the information symbol. The received average SNR at each port can be written as

$$\Gamma = \sigma^2 \frac{\mathrm{E}[|s|^2]}{\sigma_\eta^2} \equiv \sigma^2 \Theta, \tag{2}$$

where $\Theta \triangleq \frac{\mathrm{E}[|s|^2]}{\sigma_\eta^2}$ and $\sigma^2 = \mathrm{E}[|g_k|^2]$.

B. Spatial Correlation Model

The complex channels $\{g_k\}$ at the ports are spatially correlated and can be very strongly correlated because the ports can be arbitrarily close to each other when the density is high or we have a large N and small W. To characterize the correlation, in [1], [22]–[24], the first port is used as a reference as far as spatial correlation is concerned. The displacement of the k-th port from the first port can be found as

$$d_k = \left(\frac{k-1}{N-1}\right) W\lambda, \text{ for } k = 1, 2, \ldots, N. \tag{3}$$

Like the previous papers, we assume that the amplitude of the channel at each port, $|g_k|$, is Rayleigh distributed. With 2-D isotropic scattering and assuming isotropic ports, the cross-correlation function of the channel ports satisfies [28]

$$\phi_{g_k g_\ell}(d_k - d_\ell) = \frac{\sigma^2}{2} J_0\left(\frac{2\pi(k-\ell)}{N-1} W\right), \tag{4}$$

where $J_0(\cdot)$ is the zero-order Bessel function of the first kind.

With the correlation structure (4) in mind, [1], [22]–[24] model the channels at the N antenna ports by the parametric generalized spatial correlation model

$$\begin{cases} g_1 = \sigma x_0 + j\sigma y_0 \\ g_k = \sigma\left(\sqrt{1-\mu_k^2} x_k + \mu_k x_0\right) \\ \qquad + j\sigma\left(\sqrt{1-\mu_k^2} y_k + \mu_k y_0\right), k = 2, \ldots, N, \end{cases} \tag{5}$$

in which $x_0, \ldots, x_N, y_0, \ldots, y_N$ are all independent Gaussian random variables with zero mean and variance of $1/2$, and $\{\mu_k\}$ are the cross-correlation parameters that characterize the correlation of the k-th port with respect to (w.r.t.) the reference port (i.e., the first port). Also, it was proposed to set

$$\mu_k = J_0\left(\frac{2\pi(k-1)}{N-1} W\right), \text{ for } k = 2, \ldots, N. \tag{6}$$

However, the limitation of (5) and (6) is that the first port becomes the only reference point to measure spatial correlation and if two ports are weakly correlated with the first port, then it will imply that these two ports are also weakly correlated to

each other. For this reason, the above-mentioned model tends to overestimate the diversity achievable by the ports away from the first port. Additionally, if the spatial correlation between two ports in a linear structure is to be characterized properly, we should ensure the correlation parameters such that

$$\mu_k \mu_\ell = J_0\left(\frac{2\pi(k-\ell)}{N-1}W\right), \text{ for any } k, \ell. \tag{7}$$

It is clear that the condition (6) is unable to achieve (7) which reveals the weakness of the model used in [1], [22]–[24].

To address this, [2] proposes to remove the first port in (5) and set $\mu_k = \mu \ \forall k$ so that

$$g_k = \sigma\left(\sqrt{1-\mu^2}x_k + \mu x_0\right) + j\sigma\left(\sqrt{1-\mu^2}y_k + \mu y_0\right), \ k = 1, \ldots, N. \tag{8}$$

In particular, it was proposed to choose

$$\mu = \sqrt{2}\sqrt{{}_1F_2\left(\frac{1}{2}; 1, \frac{3}{2}; -\pi^2 W^2\right) - \frac{J_1(2\pi W)}{2\pi W}}. \tag{9}$$

In so doing, all the ports are tied together via μ and the spatial correlation between any two ports is modelled. Hence, every port is a reference port to any other port. Furthermore, (9) is aimed to mould the model (8) to achieve the same average correlation coefficient of what the condition (7) requires. In this paper, we use (8) and (9) to model the channels.

C. Port Selection

To achieve the best performance of fluid antenna, one needs to select the best port out of the N available ports. For single-user systems, the aim is to find the port that maximizes the received SNR, i.e.,

$$k_{\text{opt}} = \arg_k \max\left\{|g_1|, |g_2|, \ldots, |g_N|\right\}, \tag{10}$$

where k_{opt} gives the index of the optimal port. If the receiver has access to the knowledge of all the channels, $\{|g_k|\}$, then the selection will be straightforward. The challenge, however, is that N can be very large, which makes it infeasible to have the full knowledge of $\{|g_k|\}$. A more practical setting is that only a small subset of the ports are known for port selection. As a consequence, the problem (10) becomes (see Fig. 1)

$$k^* = \arg_k \max\left\{\{|g_k|\}_{k\in\mathcal{K}}, \{|\tilde{g}_k|\}_{k\in\mathcal{U}}\right\}, \tag{11}$$

where $\mathcal{K}$ denotes the set of the indices of known channel gains, $\mathcal{U}$ is the set of the indices of unknown channel gains, and $\tilde{g}_k$ represents an estimated channel at the k-th port if it has been inferred or estimated by some means. In [1], several machine learning based methods were developed to solve the problem (11), which has shown promising performance. The objective of this paper is to re-evaluate those port selection algorithms but when the channels are modelled using (8) and (9).

III. Port Selection Algorithms

The algorithms we consider are those presented in [1]. Note that the analytical approximation is no longer possible because the first port in (5) is removed. In this section, we outline the algorithms but refer the readers to [1] for more details.

A. Long Short-Term Memory (LSTM)

One method to tackle (11) is to construct an estimate of $|g_\ell|$ for all $\ell \in \mathcal{U}$ given the known channels $\{|g_k|\}_{k\in\mathcal{K}}$. To learn and exploit the correlation structure between the ports for the estimation of $\{|g_\ell|\}_{\ell\in\mathcal{U}}$, LSTM machine learning models can be useful. In particular, LSTM can treat the channels over the ports in space as a time series and supervised learning can be employed to train the LSTM model to estimate the unknown ports so that port selection can be performed. The parameters of the LSTM model we use can be found in [1, TABLE II].

B. SPO

In [1], SPO was proposed to solve (11). The advantage of SPO is that it puts the emphasis on obtaining the best estimate of the port selection, rather than the estimates of the unknown ports. The SPO approach was originally proposed in [27] and designed to perform estimation (or prediction) with emphasis on the outcome of the final optimization. In what follows, the port selection problem can be cast as

$$\mathcal{L}_{\text{spo}}(\tilde{\boldsymbol{g}}, \boldsymbol{g}) = \boldsymbol{g}^T \omega^*(\tilde{\boldsymbol{g}}) - z^*(\boldsymbol{g}), \tag{12}$$

in which $\boldsymbol{g} \triangleq [|g_1| \cdots |g_N|]^T$, $\tilde{\boldsymbol{g}} \triangleq [|\tilde{g}_1| \cdots |\tilde{g}_N|]^T$, and the superscript T denotes the transpose of a vector,

$$\omega^*(\boldsymbol{g}) = \arg\max_{\boldsymbol{x}\in\mathcal{X}} \boldsymbol{g}^T \boldsymbol{x}, \tag{13}$$

where $\mathcal{X}$ is the set of all possible N-dimensional vectors that have zeros in all dimensions except one being unity, and

$$z^*(\boldsymbol{g}) = \max_{\boldsymbol{x}\in\mathcal{X}} \boldsymbol{g}^T \boldsymbol{x}. \tag{14}$$

The first term in (12) returns the channel gain of the estimated port and the second term obtains the channel gain of the best port. In addition, as long as $\omega^*(\tilde{\boldsymbol{g}})$ outputs the correct port, it produces the true optimal solution even if some estimates of the channels deviate greatly from the true values.

To overcome the difficulty of minimizing (12), the following approximation of $\mathcal{L}_{\text{spo}}(\tilde{\boldsymbol{g}}, \boldsymbol{g})$ is considered [27]:

$$\mathcal{L}_{\text{spo+}}(\tilde{\boldsymbol{g}}, \boldsymbol{g}) = (\boldsymbol{g}^T - 2\tilde{\boldsymbol{g}}^T)\omega^*(\boldsymbol{g}^T - 2\tilde{\boldsymbol{g}}^T) + 2\tilde{\boldsymbol{g}}^T\omega^*(\boldsymbol{g}) - \boldsymbol{g}^T\omega^*(\boldsymbol{g}), \tag{15}$$

in which $\tilde{\boldsymbol{g}} = \mathbf{B}\boldsymbol{a}$ and $\boldsymbol{a}$ is the feature vector containing the channel gains of all the known ports, and $\mathbf{B}$ is an $N \times |\mathcal{K}|$ linear mapping matrix. The minimization (15) is still challenging as $\omega^*(\cdot)$ involves maximization over a discrete set. To tackle this, it is possible to replace the feasible set $\mathcal{X}$ by its convex hull without changing the optimal value of (13) and write [29]

$$\omega^*(\boldsymbol{g}) = \arg\max_{\boldsymbol{x}\in\text{conv}(\mathcal{X})} \boldsymbol{g}^T \boldsymbol{x}. \tag{16}$$

With (16), (15) can be minimized using a subgradient method, with the subgradient of (15) derived as

$$s(\tilde{\boldsymbol{g}}, \boldsymbol{g}) = 2\left[\omega^*(\boldsymbol{g}) - \omega^*(2\tilde{\boldsymbol{g}} - \boldsymbol{g})\right]. \tag{17}$$

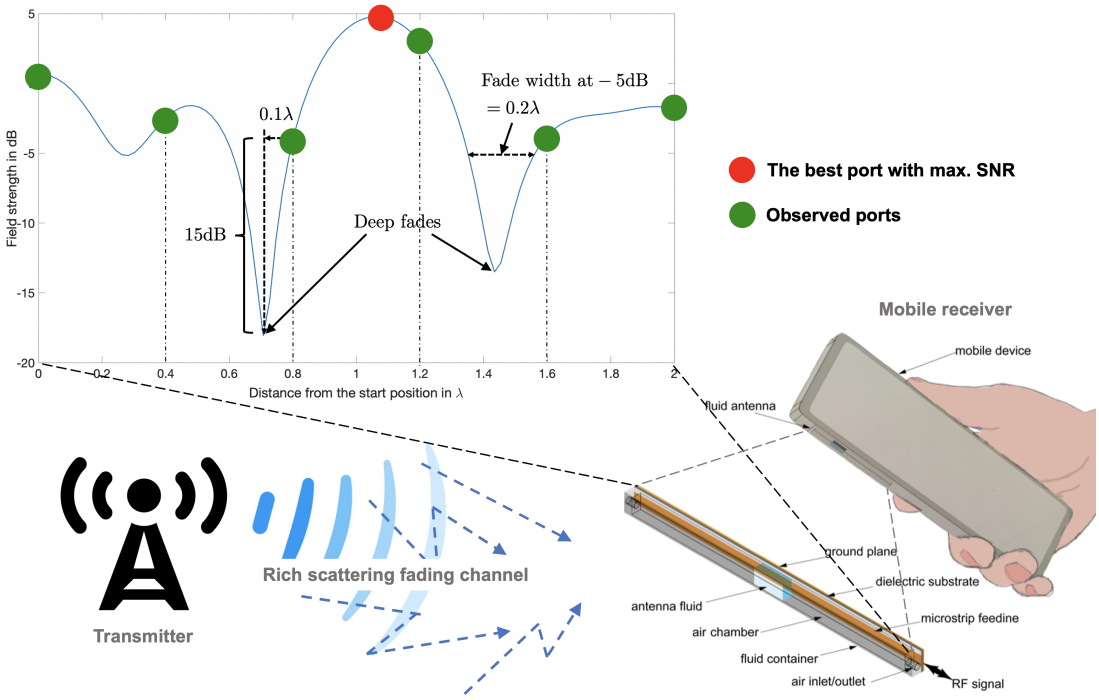

Fig. 1. Port selection for a fluid antenna system.

Overall, the port selection solution can be obtained by $\omega^*(\mathbf{B}\boldsymbol{a})$ after $\mathbf{B}$ is found by

$$\min_{\mathbf{B}\in\mathbb{R}^{N\times|\mathcal{K}|}} \sum_{i=1}^{Q} \mathcal{L}_{\text{spo+}}(\mathbf{B}\boldsymbol{a}^{(i)}, \boldsymbol{g}^{(i)}), \tag{18}$$

where Q is the batch size or the number of training examples in the dataset, $\boldsymbol{a}^{(i)}$ denotes the feature vector of the i-th sample, and $\boldsymbol{g}^{(i)}$ is i-th labelled sample. A stochastic gradient descent algorithm for updating $\mathbf{B}$ is obtained in [1, Algorithm 1].

C. SPO+LSTM

LSTM and SPO can be combined to solve (11), which we refer to it as SPO+LSTM in the results section. Given a dataset of Q labelled examples, we divide it into two datasets, half for training and half for testing SPO. The output for testing of SPO presents a crucial feature set that will be used to train and test LSTM in a concatenated manner. In particular, in our simulation results, two-third of the feature set will be used to train LSTM while the rest is used to test it.

D. Complexity Analysis

In terms of the complexity of the algorithms, it should be noted that the more the training samples, the higher the accuracy and hence the better the outage probability performance. The complexity of different algorithms has been examined in [1]. Furthermore, note that the machine learning methods are used to exploit the correlation structure of the channels over the ports and if the correlation structure somehow changes, the resulting machine learning models may become ineffective and retraining will be required. That said, the correlation structure normally does not change as the geometry of the fluid antenna remains fixed in the entire time. The statistical distribution of the fading envelope however may change depending upon the environment and the richness of scatterers.

IV. Simulation Results

A. Setup

In this section, simulation results are provided to evaluate the proposed port selection algorithms against several known benchmarks. All the wireless channels in the simulations are assumed to follow Rayleigh distributed and the fluid antenna has a linear structure with their spatial correlation between the ports modelled as (8). Moreover, the known ports in $\mathcal{K}$ were evenly spread over the space of $W\lambda$. We assume that the ports are numbered from 1 to N from one end of the fluid antenna to another end. In the simulations, we considered $N = 50$. Therefore, if $|\mathcal{K}| = 1$, then the 25^{th} port will be chosen as the known port. For $|\mathcal{K}| = 5$, the 1^{st}, 12^{th}, 25^{th}, 38^{th} and 50^{th} ports will be the known ports. Below we further list the port numbers when $|\mathcal{K}| = 10$ and $|\mathcal{K}| = 15$:

- $1, 6, 12, 17, 23, 28, 34, 39, 45, 50$;
- $1, 4, 8, 11, 15, 18, 22, 25, 29, 33, 36, 40, 43, 47, 50$.

We use 'Reference' to represent the system that chooses the best port out of the known ports for communications. It should be noted that this is not the same as the SC system with the number of uncorrelated antennas same as the number of known ports, due to the correlation between the known ports. For this reason, SC is anticipated to perform slightly better than the 'Reference' system. The other benchmarks we consider in the simulations are SC and MRC with uncorrelated antennas.

B. Results and Discussion

We provide the outage probability results for the proposed algorithms in Figs. 2–4 for $W = 0.5, 2$ and 5, respectively. A target SNR of 10 and the average SNR $\Gamma = 15$ were assumed. The proposed methods, SPO, LSTM as well as SPO+LSTM, are compared with the benchmarks. The results show that the proposed machine learning methods do work as they can bring down the outage probability, lower than the 'Reference' system for a given number of known ports (i.e., observed ports). If we compare these results with that in [1], however, the results considering the new model (8) are less impressive than that in [1] although the performance difference is insignificant when W is large. This means that (8) is more effective in considering the limitation due to strong spatial correlation for small W. That said, when $W = 0.5$, the proposed methods are still able to match the performance of many antennas. In particular, the results indicate that SPO performs the best in all the cases. For $W = 0.5$, if $|\mathcal{K}| = 5$ (i.e., 10% of the ports are known), then SPO can outperform 2-antenna MRC. If $|\mathcal{K}| = 15$, SPO even beats 3-antenna MRC and 6-antenna SC. One clear difference in the new results is that both LSTM and SPO+LSTM do not seem to work well as they do not offer noticeable performance gain over 'Reference', and only SPO works. When W is large, i.e., $W = 2, 5$, the results using the new model (8) look similar to those in [1]. In these cases, SPO is still the best but the intelligence of LSTM and SPO+LSTM begins to appear if the number of observed ports increases. Furthermore, if both W and $|\mathcal{K}|$ are large, then the machine learning based methods are particularly effective and their performance gains become more apparent. The results further demonstrate that SPO can match or exceed 6-antenna MRC if $|\mathcal{K}| = 15$ and $W = 2, 5$.

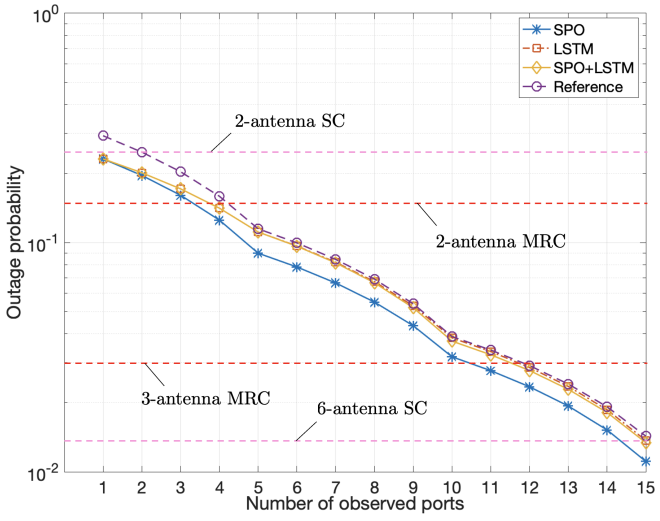

Fig. 2. Outage probability results when $W = 0.5$ and $N = 50$.

V. Conclusion

This paper revisited the port selection problem for single-user fluid antenna systems where only the channels for a subset of ports are known, and an improved spatial correlation model was used to characterize the correlation between the ports. Our contributions are the new results that confirm the performance of the proposed learning based methods for port selection. The results have demonstrated that significant reduction in outage probability can be achieved even if very few ports of the fluid antenna system are known. Moreover, SPO for port selection can match or even exceed the SC and MRC systems with many uncorrelated antennas, suggesting strongly that fluid antenna utilize the space effectively under practical conditions.

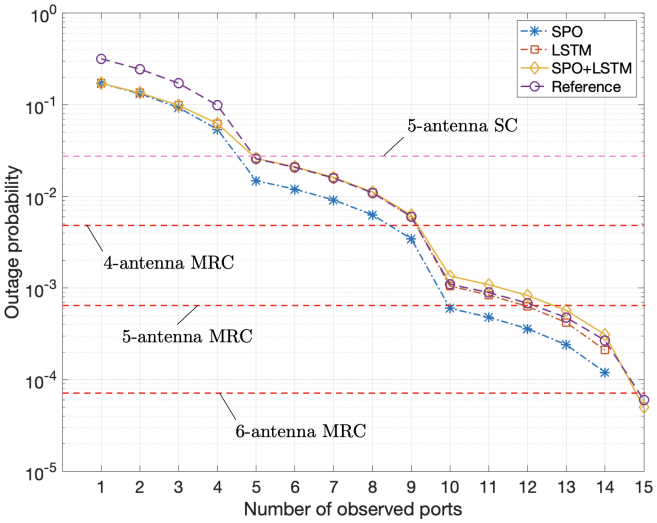

Fig. 3. Outage probability results when $W = 2$ and $N = 50$.

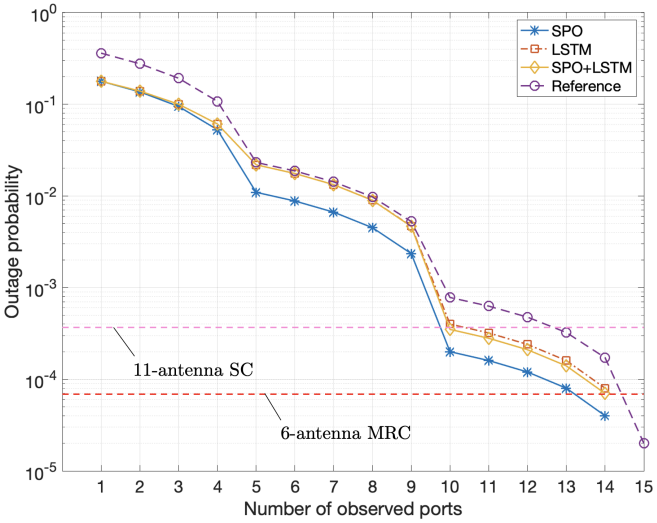

Fig. 4. Outage probability results when $W = 5$ and $N = 50$.

References

[1] Z. Chai, K. K. Wong, K. F. Tong, Y. Chen, and Y. Zhang, "Port selection for fluid antenna systems," accepted in *IEEE Commun. Letters*, 2022.

[2] K. K. Wong, K. F. Tong, Y. Chen and Y. Zhang, "Closed-form expressions for spatial correlation parameters for performance analysis of fluid antenna systems," accepted in *IET Elect. Letters*, 2022

[3] K. K. Wong, K. F. Tong, Y. Zhang, and Z. Zheng, "Fluid antenna system for 6G: When Bruce Lee inspires wireless communications," *IET Electronics Lett.*, vol. 56, no. 24, pp. 1288–1290, 26 Nov. 2020.

[4] K. K. Wong, K. F. Tong, Y. Shen, Y. Chen, and Y. Zhang, "Bruce Lee-inspired fluid antenna system: Six research topics and the potentials for 6G," accepted in *Frontiers Commun. & Netw., section Wireless Commun.*.

[5] S. J. Kar, A. Chakrabarty and B. K. Sarkar, "Fluid antennas," in *Propc. IEEE Middle East Conf. Antennas & Propag. (MECAP 2010)*, pp. 1–6, 20-22 Oct. 2010, Cairo, Egypt.

[6] Y. Kosta and S. Kosta, "Liquid antenna systems," in *Proc. IEEE Antennas & Propag. Society Symp.*, vol. 3, pp. 2392–2395, 20-25 Jun. 2004, Monterey, CA, USA.

[7] Mitsubishi Electric, *Mitsubishi electric's SeaAerial antenna uses seawater plume*, Available [online]: https://www.mitsubishielectric.com.

[8] M. Hampson, "New antenna uses saltwater and plastic to steer radio beams," *IEEE Spectrum-The Tech Talk blog*, 2019.

[9] L. Xing, J. Zhu, Q. Xu, D. Yan and Y. Zhao, "A circular beam-steering antenna with parasitic water reflectors," *IEEE Antennas & Wireless Propag. Letters*, vol. 18, no. 10, pp. 2140–2144, 2019.

[10] G. J. Hayes, J. So, A. Qusba, M. D. Dickey and G. Lazzi, "Flexible liquid metal alloy (EGaIn) microstrip patch antenna," *IEEE Trans. Antennas & Propag.*, vol. 60, no. 5, pp. 2151–2156, 2012.

[11] A. M. Morishita, C. K. Y. Kitamura, A. T. Ohta and W. A. Shiroma, "A liquid-metal monopole array with tunable frequency, gain, and beam steering," *IEEE Antennas & Wireless Propag. Letters*, vol. 12, pp. 1388–1391, 2013.

[12] A. Dey, R. Guldiken and G. Mumcu, "Microfluidically reconfigured wideband frequency-tunable liquid-metal monopole antenna," *IEEE Trans. Antennas & Propag.*, vol. 64, no. 6, pp. 2572–2576, 2016.

[13] C. Borda-Fortuny, K. Tong, A. Al-Armaghany and K. K. Wong, "A low-cost fluid switch for frequency-reconfigurable Vivaldi antenna," *IEEE Antennas & Wireless Propag. Letters*, vol. 16, pp. 3151–3154, 2017.

[14] C. Borda-Fortuny, L. Cai, K. F. Tong and K. K. Wong, "Low-cost 3D-printed coupling-fed frequency agile fluidic monopole antenna system," *IEEE Access*, vol. 7, pp. 95058–95064, 2019.

[15] A. Singh, I. Goode and C. E. Saavedra, "A multistate frequency reconfigurable monopole antenna using fluidic channels," *IEEE Antennas & Wireless Propag. Letters*, vol. 18, no. 5, pp. 856–860, 2019.

[16] B. A. Cetiner, H. Jafarkhani, Jiang-Yuan Qian, Hui Jae Yoo, A. Grau and F. De Flaviis, "Multifunctional reconfigurable MEMS integrated antennas for adaptive MIMO systems," *IEEE Commun. Mag.*, vol. 42, no. 12, pp. 62–70, 2004.

[17] A. Grau Besoli and F. De Flaviis, "A multifunctional reconfigurable pixeled antenna using MEMS technology on printed circuit board," *IEEE Trans. Antennas & Propag.*, vol. 59, no. 12, pp. 4413–4424, 2011.

[18] C. Chiu, J. Li, S. Song and R. D. Murch, "Frequency-reconfigurable pixel slot antenna," *IEEE Trans. Antennas & Propag.*, vol. 60, no. 10, pp. 4921–4924, 2012.

[19] D. Rodrigo, B. A. Cetiner and L. Jofre, "Frequency, radiation pattern and polarization reconfigurable antenna using a parasitic pixel layer," *IEEE Trans. Antennas & Propag.*, vol. 62, no. 6, pp. 3422–3427, 2014.

[20] S. Song and R. D. Murch, "An efficient approach for optimizing frequency reconfigurable pixel antennas using genetic algorithms," *IEEE Trans. Antennas & Wireless Propag.*, vol. 62, no. 2, pp. 609–620, 2014.

[21] Y. Huang, L. Xing, C. Song, S. Wang and F. Elhouni, "Liquid antennas: Past, present and future," *IEEE Open J. Antennas & Propag.*, vol. 2, pp. 473–487, 2021.

[22] K. K. Wong, A. Shojaeifard, K.-F. Tong and Y. Zhang, "Fluid antenna systems," *IEEE Trans. Wireless Commun.*, vol. 20, no. 3, pp. 1950–1962, Mar. 2021.

[23] K. K. Wong, A. Shojaeifard, K.-F. Tong and Y. Zhang, "Performance limits of fluid antenna systems," *IEEE Commun. Lett.*, vol. 24, no. 11, pp. 2469–2472, Nov. 2020.

[24] K. K. Wong, and K.-F. Tong, "Fluid antenna multiple access," accepted in *IEEE Trans. Wireless Commun.*, 2022.

[25] K. K. Wong, D. Morales-Jiménez, and K.-F. Tong, "Slow fluid antenna multiple access," submitted to *IEEE Trans. Wireless Commun.*, 2022.

[26] Y. Shen, K. F. Tong, and K. K. Wong, "Beam-steering surface wave fluid antennas for MIMO applications," in *Proc. The 2020 Asia-Pacific Microwave Conf. (APMC 2020)*, 8-11 Dec. 2020, Hong Kong, China.

[27] A. N. Elmachtoub and P. Grigas, "Smart 'predict, then optimize'," *Management Science*, 2021, doi: 10.1287/mnsc.2020.3922.

[28] G. L. Stüber, *Principles of Mobile Communication*, Second Edition, Kluwer Academic Publishers, 2002.

[29] M. Jaggi, "Convex optimization without projection steps," [Online] arXiv preprint arXiv:1108.1170, 2011.